Transfer of an Erbium Ion across the Water/Dodecane Interface: Structure and Thermodynamics via Molecular Dynamics **Simulations** 

John J. Karnes, a,b Nathan Villavicencio and Ilan Benjamin \*\*

a) Department of Chemistry and Biochemistry, University of California, Santa Cruz,

1156 High Street, California 95064, USA

b) Materials Engineering Division, Lawrence Livermore National Laboratory,

7000 East Avenue, Livermore California 94550, USA

The thermodynamics and structural changes involved in the transfer of the Er<sup>3+</sup> ion across the

water/dodecane interface are investigated by molecular dynamics simulations. We show that the

Er3+ ion is transferred as a highly conserved 8-water coordinated species and that the transfer

involves significant perturbation of the interfacial water structure. Several structural properties are

used to quantify this process. Implications for the ion extraction process are discussed.

\* Email address: ilan@ucsc.edu

1

#### 1. Introduction

The transfer of metal ions from an aqueous to an organic phase is important for environmental remediation, mining of rare earth metals, and the extraction of radionuclides from nuclear waste [1-3]. In the process of solvent extraction, organic molecules (extractants) assist the transfer of metal ions from an aqueous to an organic phase. For example, an amphiphilic extractant molecule with a phosphoric acid head group can strongly bind to metal ions. The extractant's hydrophobic alkyl tail group makes it soluble in the organic phase, facilitating phase transfer. These ion-extractant coordination complexes or reverse micelles are two approaches that may be utilized to promote the transfer of aqueous ions into an adjacent organic phase [4, 5].

While the interaction of metal ions with extractants at the organic-aqueous interface is likely an important factor determining the efficiency and kinetics of extraction [6], the mechanism of the ion transfer across the interface is not well understood. In particular, it is not known how highly charged ions that are strongly coordinated with 6-8 water molecules in the aqueous phase are extracted with only few co-extracted water molecules [7]. There is some evidence that water density fluctuations in the form of "fingers" play an important role [8-10]. For example, it has been suggested that DEHP (bis(2-ethylhexyl)phosphoric acid) extractant can form complexes with aqueous metal ions when fingers of water reach into the organic phase [11].

Clearly, a combination of experimental and theoretical approaches is critical for elucidating the molecular mechanism of solvent extraction [7, 12, 13]. We and others have extensively studied the mechanism of ion and ion-pair transfer across the liquid/liquid interface [8-10, 14-17]. An important conclusion of these studies has been that taking into account water surface fluctuations during ion transfer and the partial co-transfer of the ion hydration shell is crucial for correctly describing the ion transfer mechanism. However, not much work has been done to

examine these aspects with highly charged ions. The purpose of this letter is to provide a fundamental understanding of the behavior of the Er<sup>3+</sup> ion at the water/dodecane interface as an example of a highly charged ion of current experimental interest [7]. These calculations can be used to validate the intermolecular potentials that will be used to simulate the full extraction process and provide benchmark behavior of the system without the extractants present.

# 2. Systems and methods

The water/dodecane liquid/liquid interfacial system consists of two adjacent slabs of 2490 water molecules and 320 dodecane molecules in a 50 Å  $\times$  50 Å  $\times$  300 Å rectangular box. The liquid/liquid interface is located in the *X-Y* plane at  $Z \approx 0$ , with the water phase in the region Z < 0 and the dodecane phase in the Z > 0 region (see density profiles in Figure 1 below). Each liquid phase is in equilibrium with its respective vapor phase; only one liquid/liquid interface is present. Periodic boundary conditions are applied in all directions and a soft reflecting potential wall is located 5 Å from the simulation box boundaries in the *Z*-direction to prevent molecules from crossing into the adjacent vapor phase.

The single  $Er^{3+}$  cation is placed in 22 different 3 Å-wide overlapping windows, spanning the region from Z = -10 Å (bulk water) to Z = +30 Å. Neighboring windows overlap by 1 Å. In each window a 2 ns constant temperature (T = 298 K) Molecular Dynamics (MD) trajectory is obtained, which allows for statistically accurate calculations of different structural properties of the cation as a function of the distance from the interface. The MD simulations are performed with our inhouse software that uses the velocity Verlet algorithm with an integration time-step of 1 fs.

The intermolecular interaction potentials are represented as the pairwise sum of Lennard-Jones (LJ) and coulomb terms

$$u_{ij} = 4\varepsilon_{ij} \left[ \left( \frac{\sigma_{ij}}{r} \right)^{12} - \left( \frac{\sigma_{ij}}{r} \right)^{6} \right] + \frac{q_i q_j}{4\pi r \varepsilon_0} \,, \tag{1}$$

where r is the distance between atom centers i and j. Standard Lorentz-Berthelot combining rules,  $\sigma_{ij} = (\sigma_i + \sigma_j)/2$  and  $\varepsilon_{ij} = (\varepsilon_i \, \varepsilon_j)^{1/2}$ , are used to generate Lennard-Jones parameters for all mixed interactions. For water we use a version of the flexible SPC model with intramolecular potentials as described by Kuchitsu and Morino [18]. The dodecane molecules are modeled using the OPLS-UA force field with all the needed parameters given in reference [19]. The Er³+ parameters were taken from the IOD (ion-oxygen distance) potential in reference [20]. To validate this choice of ion parameters, several structural properties calculated in bulk water are in reasonable agreement with experiments (see below). In addition, the absolute hydration free energy calculated with these potentials using the standard integration method [21],  $\Delta G_{hyd}(calc.) = -816$  kcal/mol compares very well with the experimental value  $\Delta G_{hyd} = -838$  kcal/mol [22].

Force fields that include an empirical approach toward polarizability or directly employ some variation of QM/MM may achieve greater accuracy at significantly greater computational expense and have been shown to reveal insights into ion solvation that may not be obtained with fixed-charge force fields.[23-25] The fixed charged, coarse-grained model employed and validated in this work meets our desired level of thermodynamic and structural accuracy and will permit future, related studies of ion transfer in significantly more complex extraction environments while still remaining within the reach of moderate computational resources. Polarization effects due to the highly charged erbium ion would be most dramatic in nonpolar media like dodecane, but these interactions would also be heavily screened by the large hydrations shells that accompany the Er<sup>3+</sup>

through these simulations. The empirical parameterization of SPC water does account for charge screening, as evidenced by its reduced effective dipole of  $\mu^{\rm eff} \approx 2.3$  D versus a value of  $\mu_l \approx 3$  D as reported in *ab initio* and experimental studies. Leontyev and Stuchebrukhov have shown[26] that this effective dipole may be understood as the scaling by the square root of the high frequency dielectric constant of water,  $\mu^{\rm eff} = \mu_l/\sqrt{\varepsilon_{\rm el}}$ , where  $\varepsilon_{\rm el} = 1.78$  for water, a relationship extended to yield the electronic continuum correction (ECC).[27-29]

The free energy profile for the transfer of the ion across the interface is determined using the average force integration method [30]. Denoting by F(z) the ensemble average of the total projected force along the interface normal on the ion fixed at the position z along the interface normal, the potential of mean force A(Z) at the position Z relative to a point  $Z_W$  in bulk water is given by

$$A(Z) = -\int_{Z_W}^Z F(z) dz. \tag{2}$$

The ion is held fixed at different z locations (by setting the Z-components of the force on the ion and the velocity of the ion to zero each time step) that are spaced closely enough to get a smooth function F(z).

### 3. Results and discussion

The free energy profile for the transfer of the  $Er^{3+}$  ion across the water/dodecane interface is shown in Figure 1. Superimposed on the same panel are the density profiles of water and dodecane calculated from a simulation where the  $Er^{3+}$  is in bulk water. Z=0 is the location of the Gibbs Dividing Surface (GDS), which is the plane parallel to interface where the water density is approximately 50% of the bulk value. For an expanded discussion of the exact definition of the GDS, we refer the reader to reference [31]. The interface region (defined as the distance over which

the density of water varies from 90% to 10% of the bulk value) is quite narrow at about 5.1 Å. However, as we will see below when the ion is at the interface, significant perturbation of the interface is observed. The properties of the neat water/dodecane interface have been described in detail elsewhere.[32]

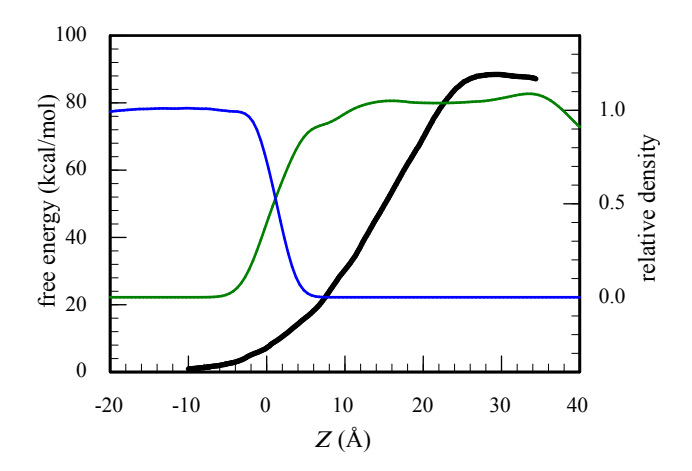


**FIG. 1**. The potential of mean force for the transfer of Er<sup>3+</sup> across the water/dodecane interface (thick black line with values shown on the left axis). The relative (to the bulk) densities of water (blue) and dodecane (green) are shown on the right axis.

The free energy profile monotonically increases as the ion is transferred across the interface to bulk dodecane. The net free energy of transfer is about 90 kcal/mol. The error estimate based on 1 standard deviation of the calculated average forces is about 4 kcal/mol. This large free energy of transfer is still significantly less than the difference between the hydration free energy and the solvation free energy of the "naked" ion in dodecane (about -10 kcal/mol), signifying that significant amount of water is co-transferred with the ion, as has been extensively demonstrated for monovalent ions [33, 34]. Furthermore, unlike the free energy profile of monovalent ions [10, 24, 35], here the free energy profile is significantly broader than the density profile. Even more

dramatic is the fact that the profile's center point is significantly shifted toward the organic phase relative to the GDS. Specifically, the free energy begins to rise as the water density starts to fall from its bulk value, reaches only about a third of the final value when the average water density is zero and finally reaches a plateau at around Z = 30 Å. This behavior is a direct consequence of the significant perturbation of the interfacial water structure caused by the significant drag of water molecules with the ion. A simulation snapshot demonstrating this perturbation when the ion is located at Z = 26 Å is shown in Figure 2.

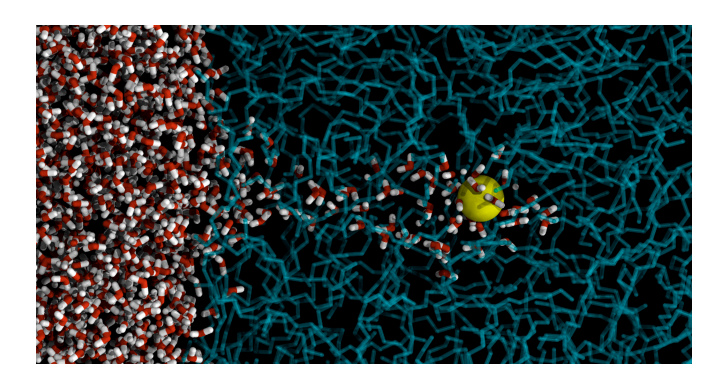


**FIG. 2.** A snapshot of the Er<sup>3+</sup> ion (yellow ball near right edge) transferred into the dodecane phase showing a significant perturbation of the water interface structure.

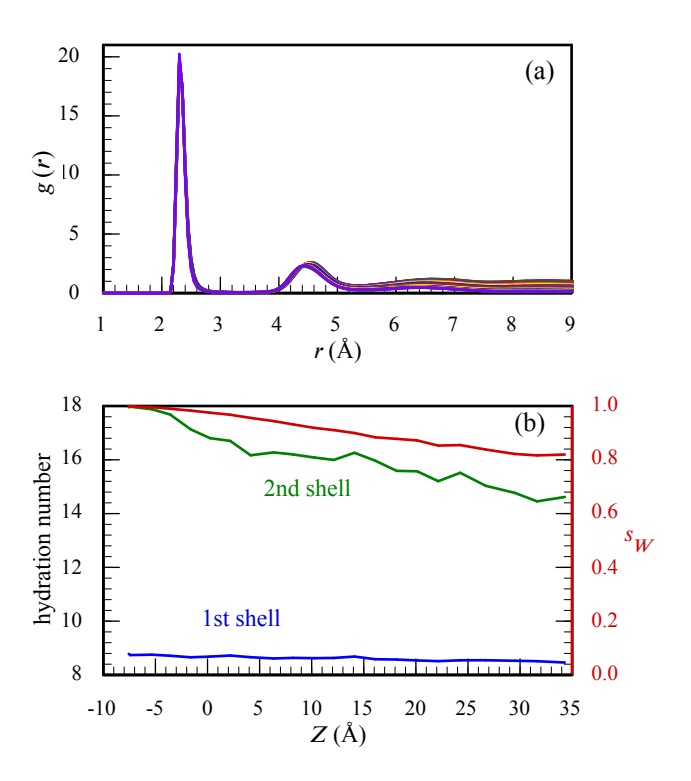


**FIG. 3.** a) The water oxygen –  $Er^{3+}$  atomic radial distributions functions for the  $Er^{3+}$  ion located in all the different windows. b) Left axis: first and second shell hydration numbers as a function of the location of the ion along the interface normal. Right axis: The ion–water interaction energy normalized by its value in bulk water.

A quantitative account of the degree of the co-transfer of water molecules with the ion is provided by examining the water-ion radial distribution functions. These functions are calculated in all 22 windows and are shown in panel (a) of Figure 3. These functions nearly exactly fall on top of each other for the first and (to slightly lesser degree) the second peak. The main distinguishing feature is their "asymptotic" (at r = 9 Å) values (1 when the ion is in bulk water and 0.5 when it is near the Gibbs surface), which simply reflects the average density of water in a spherical shell 9 Å away from the ion. A clearer view of the changing value of the radial

distribution functions can be obtained by calculating the average number of water molecules surrounding the ion:

$$\langle n(r)\rangle = \int_0^r 4\pi \rho_W g(r) r^2 dr , \qquad (3)$$

where  $\rho_W$  is the bulk water density (0.0334 Å<sup>-3</sup>). The value of the integral at the first minimum of g(r) ( $R_{\min} = 3.5$  Å) determines the ion's coordination number  $n_c$ . As panel (b) of Figure 3 demonstrates, the fact that the first peak of g(r) is nearly conserved for all locations of the ion results in a nearly constant hydration number of 8.5, which compares quite favorably with the experimental value of 8.2 in bulk water [22]. The second peak somewhat diminishes as the ion is transferred to the organic phase, with a second hydration number n(r = 5.35 Å) that corresponds to an additional six water molecules when the ion is in bulk dodecane.

Panel (b) also depicts the normalized ion-water interaction energy as another measure of the changing state of the ion. Shown as a function of the ion location is the value

$$s_W = \langle U_{I-W} \delta(Z - z_I) \rangle / U_{I-W}^{\text{bulk}}, \tag{4}$$

where  $U_{I-W}$  is the total interaction energy of the ion with water when the ion is located at some position  $z_I$ , while the quantity with the "bulk" superscript denotes the interaction energy of the ion with bulk water. The value  $U_{I-W}^{\text{bulk}} = -1382 \pm 25 \text{ kcal/mol}$  is obtained from a simulation where  $\text{Er}^{3+}$  is in bulk water. The ensemble average in Eq. 4 is over all solvent positions while the ion is at the position  $z_I$  so that  $s_W$  is a dimensionless quantity implicitly dependent on the ion's location  $z_I$  and has the values:  $s_W(z_I \square \text{ bulk water}) = 1$ ,  $s_W(z_I \square \text{ bulk dodecane}) = f$ , where f < 1 represents the interaction of the ion with (mostly) the fraction of the extended hydration shell that was cotransferred into the organic phase ( $f \approx 0$  for a hydrophobic ion). In the case of this highly charged ion,  $f \approx 0.8$ . The relatively small decline in  $s_W$  observed in panel (b) is due to the diminishing

second shell and beyond, but is less pronounced than the decline in the second hydration shell number because the contribution of the water first hydration shell to the interaction energy is nearly fixed at about  $-686 \pm 29$  kcal/mol (about 50% of the bulk value).

The conservation of the ion's hydration shell and the co-transfer of water molecules as the ion crosses the interface gives rise to the formation of water protrusions (as illustrated in Figure 2). As a result, the coordinate  $z_I$  specifying the location of the ion relative to the average location of the Gibbs surface does not provide full information about the actual hydration state of the ion. Kikkawa et. al. have suggested a "water finger coordinate" labeled w, to describe the effective separation of the ion from the bulk aqueous phase [8]. At each system configuration, the ion position and the water molecules' positions (center of mass or the oxygen atoms) represent the vertices of an undirected graph whose edges are the geometrical distances between the vertices. A connected path between the ion and bulk water is defined by the requirement that all edges along the path are shorter than a threshold distance. The coordinate w is defined to be the minimum threshold distance that give rise to a connected path. When the ion is in bulk water  $\langle w \rangle$  is approximately equal to the location of first peak of the O-O radial distribution function (or the ionoxygen RDF peak position, if longer) regardless of the position  $z_I$  of the ion. When the ion is in the organic phase connected via an un-broken water "finger" to the aqueous phase, w is approximately equal to the O-O distance corresponding to the longest hydrogen bond in the protrusion (about 3.2 Å). As the water "finger" breaks, w corresponds to the distance between the two nearest water oxygen – one that belong to the ion hydration shell and one to the water phase. In the 22 windows studied, with the ion restricted to a narrow Z range, no breakup events are observed in the 2 ns simulations when the ion is located in any region for which Z < 25 Å. A few

water "finger" breakup and re-attachment events are observed when the ion is located in the window 25 Å < Z < 28 Å and significantly more in the next window, 27 Å < Z < 30 Å. An example trajectory showing the water "finger" breakup is shown in Figure 4.

The breakup of the water finger occurs when the ion is significantly further into the organic phase than previous related studies of monovalent chloride where the water finger breakup occurs when the ion about 12 Å away from the GDS into the organic phase.[8, 10, 36] It is important to note three key features of the longer water finger in the Er<sup>3+</sup> system. First, the absolute length of the water finger structure cannot be accurately intuited from  $z_I$  alone. Since  $Er^{3+}$  transfers with a reasonably stable cluster that contains most of its first and second hydration shells, the width of these hydration shells themselves contribute to the larger value of  $z_l$ . Second, the co-transfer of  $Er^{3+}$ 's hydration shells also make the transferring complex larger in the X and Y dimensions, resulting in the formation of an inherently wider "finger" that remains several water molecules wide as the ion moves toward the organic phase. This larger characteristic aspect ratio of the water finger structure, which can be more accurately described as a water "cone", also accounts for its ability to remain intact at greater values of  $z_l$ . Finally, it is important to note that the breakup of water fingers is more likely in a relatively high dielectric constant medium (like nitrobenzene used in the above studies) whose molecules can form hydrogen bonds with water molecules. This is unlike the present case of the highly hydrophobic dodecane, which further explains the stability of long water "fingers".

The fact that finger breakup begins to take place when the water finger extends 2.5 nm into the organic phase is another factor contributing to the fact that the free energy of transfer is much smaller than the difference between the solvation free energy of the ion in water and the "naked" ion in dodecane: The ion is able to maintain a favorable hydration environment deep into the

organic phase. Indeed, calculations of free energy of transfer of a hydrated ion cluster while the interface is constrained to remain flat (no protrusions) in a different system resulted in a significant increase in the free energy of transfer [10].

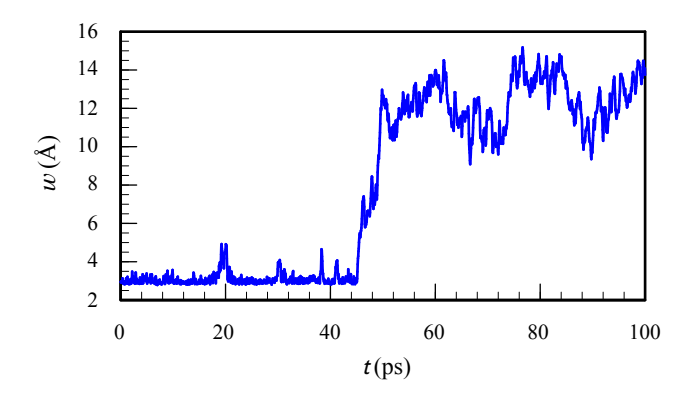


**FIG. 5.** A trajectory segment showing a water "finger" breakup event while the  $Er^{3+}$  ion is constrained to a window 25 Å <  $z_I$  < 28 Å. The coordinate w is equal to the minimum threshold distance that will give rise to a connected path between the ion and bulk water [8].

Extensive sampling of the coordinate w using a 8 ns trajectory when the ion is constrained to be in the region 25 Å < Z < 28 Å allows us to compute the free energy profile along this coordinate, shown in Figure 5.

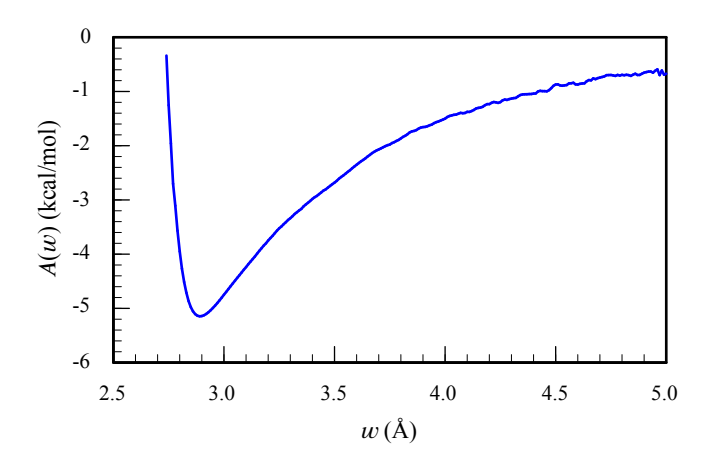


**FIG. 5.** The potential of mean force along the water "finger" coordinate w while the ion's Z position along the interface normal is constrained to a 3 Å-wide slab whose center is located 26 Å "above" the Gibbs surface.

The equilibrium value of w (corresponding to the minimum of the PMF in Figure 5) at 2.9 Å is only slightly larger than the peak position of the O-O radial distribution function in bulk SPC water [37]. The free energy cost to increase w to the value *defined* to be the maximum hydrogen bond length [38-41], 3.4 Å, is close to the accepted value of hydrogen bond energy [41] of about 2.5 kcal/mol. However, the total well depth of the PMF in Figure 5 is approximately 5 kcal/mol. The additional 2.5 kcal/mol represents the free energy associated with increasing w up to about 6 Å where the PMF reaches a near plateau. This additional free energy represents the work done to drive the hydrated ion away from the interface as well as the return of the extended water protrusion to the neat equilibrium structure once the ion is away from the interface.

The considerable perturbation of the interface structure and increased width which accompanies the ion transfer can be demonstrated by calculating the excess the number of water molecules in the organic phase  $NW_{\text{excess}}$  as a function of the ion location  $Z_1$ . This can be determined from the water density profile as follows:

$$\langle NW_{\text{excess}}\rangle(Z_I) = A \int_{Z_G}^{Z_D} [\rho_{neat}(z) - \rho(z; Z_I)] dz, \qquad (5)$$

where  $\rho_{\text{neat}}(z)$  is the neat water density profile (no ion),  $\rho(z; Z_I)$  is the density profile of water when the ion is (restricted to the lamella) at an average location  $Z_I$ ,  $z_G$  is the location of the Gibbs

surface determined from the relation  $\rho(z_G; Z_I) = 0.5$ ,  $z_D$  is a location in bulk dodecane where the water density reaches zero:  $\rho(z_D; Z_I) = 0$  and A is the simulation box surface area.

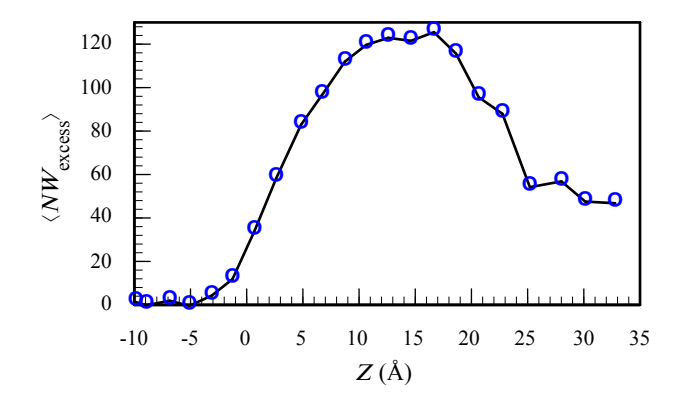


**FIG. 6**. Average number of excess water molecules in the organic phase as a function of the Er<sup>3+</sup> ion location.

Figure 6 demonstrates that the ion transfer gives rise to considerable perturbation of the interface as the number of water molecules in the organic phase is significantly larger than the number of molecules in the first and second hydration shells (compare with Figure 3b). This number reaches a maximum when the ion is near 15 Å, which represents a thick water "cone" with the ion at its tip. The number begin to drop as the "cone" is thinning and becoming a "finger"-like structure and finally, when the ion breaks away from the bulk water, there are still 44 - 8 - 14 = 22 water molecules outside the second shell.

### 4. Conclusions

The  $Er^{3+}$  cation is transferred across the interface as a highly conserved  $Er(H_2O)8^{3+}$  species. The free energy of transfer  $\Delta G_t$  is very large, clearly demonstrating the need for an extracting agent. However,  $\Delta G_t$  is much smaller than the difference between the solvation free

energy of the ion in water and the "naked" ion in dodecane. This is due to the significantly smaller free energy of transfer of the  $Er(H_2O)8^{3+}$  species and the fact that the transfer takes place deep into the organic phase, facilitated by water protrusions. This can enable an extracting molecule that is located in the bulk organic phase to interact with the cation. Future work will examine the free energy of binding of the metal ion with extractant molecules at this location and the necessary exchange of hydration shell water molecules that must accompany this binding.

## Acknowledgments

This work was supported by the National Science Foundation through grant CHE-1800158. [NV, IB] This work was performed under the auspices of the U.S. Department of Energy by Lawrence Livermore National Laboratory under Contract DE-AC52-07NA27344 [JJK]

### References

- [1] M. Cox, M. Hidalgo, M. Valiente, Solvent Extraction for the 21st Century, SCI, London, 2001.
- [2] K.L. Nash, G.J. Lumetta, S.B. Clark, J. Friese, Significance of the nuclear fuel cycle in the 21st century, ACS Sym. Ser. 933 (2006) 3-20.
- [3] A.M. Wilson, P.J. Bailey, P.A. Tasker, J.R. Turkington, R.A. Grant, J.B. Love, Solvent extraction: the coordination chemistry behind extractive metallurgy, Chem. Soc. Rev. 43 (2014) 123-134.
- [4] D.C. Steytler, T.R. Jenta, B.H. Robinson, J. Eastoe, R.K. Heenan, Structure of reversed micelles formed by metal salts of bis(ethylhexyl) phosphoric acid, Langmuir 12 (1996) 1483-1489.

- [5] R.J. Ellis, T.L. Anderson, M.R. Antonio, A. Braatz, M. Nilsson, A SAXS Study of Aggregation in the Synergistic TBP-HDBP Solvent Extraction System, J. Phys. Chem. B 117 (2013) 5916-5924.
- [6] P.R. Danesi, R. Chiarizia, The Kinetics of Metal Solvent-Extraction, CRC Current Rev. Anal. Chem. 10 (1980) 1-126.
- [7] Z. Liang, W. Bu, K.J. Schweighofer, D.J. Walwark, Jr., J.S. Harvey, G.R. Hanlon, D. Amoanu, C. Erol, I. Benjamin, M.L. Schlossman, Nanoscale view of assisted ion transport across the liquid-liquid interface, Proc. Natl. Acad. Sci. USA (2018).
- [8] N. Kikkawa, L.J. Wang, A. Morita, Microscopic Barrier Mechanism of Ion Transport through Liquid-Liquid Interface, J. Am. Chem. Soc. 137 (2015) 8022-8025.
- [9] I. Benjamin, Reactivity and Dynamics at Liquid Interfaces, Rev. Comput. Chem. 28 (2015) 205-313.
- [10] J.J. Karnes, I. Benjamin, Geometric and energetic considerations of surface fluctuations during ion transfer across the water-immiscible organic liquid interface, J. Chem. Phys. 145 (2016).
- [11] B.F. Qiao, J.V. Muntean, M.O. de la Cruz, R.J. Ellis, Ion Transport Mechanisms in Liquid-Liquid Interface, Langmuir 33 (2017) 6135-6142.
- [12] H. Watarai, S. Tsukahara, H. Nagatani, A. Ohashi, Interfacial nanochemistry in liquid-liquid extraction systems, B Chem. Soc. Jpn. 76 (2003) 1471-1492.
- [13] G. Benay, G. Wipff, Liquid-Liquid Extraction of Uranyl by TBP: The TBP and Ions Models and Related Interfacial Features Revisited by MD and PMF Simulations, J. Phys. Chem. B 118 (2014) 3133-3149.

- [14] I. Benjamin, Molecular structure and dynamics at liquid-liquid interfaces, Annu. Rev. Phys. Chem. 48 (1997) 401.
- [15] T.M. Chang, L.X. Dang, Recent advances in molecular simulations of ion solvation at liquid interfaces, Chem. Rev. 106 (2006) 1305-1322.
- [16] R.A.W. Dryfe, The Electrified Liquid-Liquid Interface, Adv. Chem. Phys. 141 (2009) 153-215.
- [17] D.J. dos Santos, J.A. Gomes, Molecular dynamics study of the calcium ion transfer across the water/nitrobenzene interface, Chem. Phys. Chem. 3 (2002) 946-951.
- [18] K. Kuchitsu, Y. Morino, Estimation of anharmonic potential constants. II. Bent XY2 molecules, Bull. Chem. Soc. Jpn. 38 (1965) 814-824.
- [19] W.L. Jorgensen, J.D. Madura, C.J. Swenson, Optimized intermolecular potential functions for liquid hydrocarbons, J. Am. Chem. Soc. 106 (1984) 6638.
- [20] P. Li, L.F. Song, K.M. Merz, Jr., Parameterization of highly charged metal ions using the 12-6-4 LJ-type nonbonded model in explicit water, J. Phys. Chem. B 119 (2015) 883-895.
- [21] P. Kollman, Free-Energy Calculations Applications to Chemical and Biochemical Phenomena, Chem. Rev. 93 (1993) 2395-2417.
- [22] Y. Marcus, Ion Solvation, Wiley, New York, 1985.
- [23] L.X. Dang, T. Chang, Molecular mechanism of ion binding to the liquid/vapor interface of water, J. Phys. Chem. B. 106 (2002) 235.
- [24] P. Jungwirth, D.J. Tobias, Specific ion effects at the air/water interface, Chem. Rev. 106 (2006) 1259-1281.
- [25] A. Muralidharan, L.R. Pratt, M.I. Chaudhari, S.B. Rempe, Quasi-Chemical Theory for Anion Hydration and Specific Ion Effects: Cl<sup>-</sup>(aq) vs. F<sup>-</sup>(aq), Chem. Phys. Lett. X 4 (2019) 100037.

- [26] I. Leontyev, A. Stuchebrukhov, Accounting for electronic polarization in non-polarizable force fields, Phys. Chem. Chem. Phys. 13 (2011) 2613-2626.
- [27] M. Kohagen, P.E. Mason, P. Jungwirth, Accounting for Electronic Polarization Effects in Aqueous Sodium Chloride via Molecular Dynamics Aided by Neutron Scattering, J. Phys. Chem. B 120 (2016) 1454-1460.
- [28] E. Pluharova, P.E. Mason, P. Jungwirth, Ion Pairing in Aqueous Lithium Salt Solutions with Monovalent and Divalent Counter-Anions, J. Phys. Chem. A 117 (2013) 11766-11773.
- [29] P.E. Mason, E. Wernersson, P. Jungwirth, Accurate Description of Aqueous Carbonate Ions: An Effective Polarization Model Verified by Neutron Scattering, J. Phys. Chem. B 116 (2012) 8145-8153.
- [30] E. Darve, A. Pohorille, Calculating free energies using average force, J. Chem. Phys. 115 (2001) 9169-9183.
- [31] J.S. Rowlinson, B. Widom, Molecular Theory of Capillarity, Clarendon, Oxford, 1982.
- [32] J. Chowdhary, B.M. Ladanyi, Water-Hydrocarbon Interfaces: Effect of Hydrocarbon Branching on Interfacial Structure, J. Phys. Chem. B 110 (2006) 15442-15453.
- [33] I. Benjamin, Structure and dynamics of hydrated ions in a water-immiscible organic solvent, J. Phys. Chem. B 112 (2008) 15801-15806.
- [34] D. Rose, I. Benjamin, Free energy of transfer of hydrated ion clusters from water to an immiscible organic solvent J. Phys. Chem. B 113 (2009) 9296-9303.
- [35] C.D. Wick, L.X. Dang, Molecular dynamics study of ion transfer and distribution at the interface of water and 1,2-dichlorethane, J. Phys. Chem. C. 112 (2008) 647-649.
- [36] N. Kikkawa, L. Wang, A. Morita, Computational study of effect of water finger on ion transport through water-oil interface, J. Chem. Phys. 145 (2016) 014702.

- [37] H.J.C. Berendsen, J.R. Grigera, T.P. Straatsma, The Missing Term in Effective Pair Potentials, J. Phys. Chem. 91 (1987) 6269-6271.
- [38] M.G. Sceats, S.A. Rice, The Water-Water Pair Potential near the Hydrogen-Bonded Equilibrium Configuration, J. Chem. Phys. 72 (1980) 3236-3247.
- [39] M. Mezei, D.L. Beveridge, Theoretical-Studies of Hydrogen-Bonding in Liquid Water and Dilute Aqueous-Solutions, J. Chem. Phys. 74 (1981) 622-632.
- [40] A. Luzar, D. Chandler, Hydrogen-Bond Kinetics in Liquid Water, Nature 379 (1996) 55-57.
- [41] R. Kumar, J.R. Schmidt, J.L. Skinner, Hydrogen bonding definitions and dynamics in liquid water, J. Chem. Phys. 126 (2007) 204107-204101-204107-204112.